THE JOURNAL OF PHYSICAL CHEMISTRY C

Article

Cite This: J. Phys. Chem. C 2019, 123, 24165−24171

pubs.acs.org/JPCC

Wrinkling of an Enteric Coating Induced by Vapor-Deposited Stimuli-Responsive Hydrogel Thin Films

Fabian Muralter,*[,†] Anna Maria Coclite,[†] and Oliver Werzer[‡]

[†]Institute for Solid State Physics, NAWI Graz, Graz University of Technology, 8010 Graz, Austria

[‡]Institute of Pharmaceutical Science, Department of Pharmaceutical Technology, University of Graz, 8010 Graz, Austria

ABSTRACT: In this contribution, we report on the thin-film synthesis of a thermoresponsive polymer onto another polymer used as an enteric coating in drug applications. In particular, we deposit cross-linked poly(*N*-vinylcaprolactam) (pNVCL) thin films by initiated chemical vapor deposition (iCVD) onto spin-coated Eudragit (EUD) layers. Already upon iCVD synthesis, the layered structure starts to form wrinkles at a minimum iCVD thickness of 30 nm. By changing the EUD layer thickness and the amount of cross-linking used during iCVD, the morphology of the wrinkles is demonstrated to be readily tunable. Laterally, the double-layer structures vary in morphology from being ultrasmooth to exhibiting up to a 3.5 μm wrinkle wavelength. The surface roughness and, thus, the wrinkles' height can be tailored from below 1 nm up to 100 nm. From the resulting wavelength of wrinkles, an estimation of the elastic modulus of pNVCL proves its tunability over a wide range of values thanks to the iCVD process. This study elucidates an uncomplicated way to tune the wrinkles' morphology and, thus, the surface area of a system that can be employed in drug delivery applications. Hence, an enteric coating of EUD together with an iCVD-synthesized thermoresponsive thin film is proposed as a promising composite encapsulation layer to outperform established systems in terms of tunability of the response to multiple external stimuli.

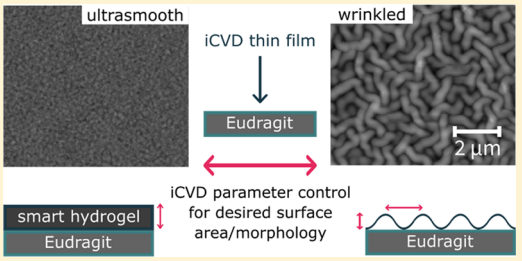

INTRODUCTION

Besides fundamental interest in wrinkling, wrinkled structures are used in applications, where an enhancement of the surface area yields superior device performance. In photovoltaics, a larger contact area in pn-junctions allows for accessing higher currents, while structures used for light scattering would also enhance energy harvesting.[1,2] In biomedical applications, the larger areas produced by wrinkles are, according to Noyes−Whitney, responsible for higher dissolution rates and, thus, enable faster drug release.[3]

Wrinkling occurs in many situations in nature[4] or can be artificially employed.[5] While the former might display its consequences meeting the needs of specific purposes, the man-made induction of wrinkles allows for studying the fundamental mechanisms in more detail. Very often, a substrate is coated by another substance so that both form a strong connection.[6] Upon changing some environmental parameters such as temperature or pressure, the response of both will be distinct; differences in expansion might result in cracks,[7] while compression of some flexible material, eventually, induces wrinkling.[8] Typical examples are metal layers on compliant substrates.[9] For polymeric samples, such behavior is often observed on prestrained substrates; depositing a coating onto the strained substrate and, subsequently, releasing the strain causes the structure to wrinkle. Employing anisotropic strain and release might even result in the formation of directed wrinkles.[10] Recently, isotropic wrinkle formation was also found to occur during the preparation of drug encapsulation layers employing a chemical vapor deposition (CVD) technique; the results showed that wrinkling occurs even without prestraining the substrate and, thus, directly upon coating an amorphous drug.[11] While the direction of the wrinkles is not adjustable, the wrinkles' size (height and wavelength) were clearly dependent on the thickness of the encapsulated layer. Further, the nature of the solid state of the encapsulated drug layer directly influenced the capability of wrinkle formation; while crystalline drug layers prevented the formation of wrinkles, an amorphous state was observed to induce wrinkled structures. Also, the chemical composition of the CVD coating had an impact not only on the wrinkle formation[12] but also on the stabilization of the amorphous state of the drug in general.[13]

Employing initiated chemical vapor deposition (iCVD) as a solvent-free process allows for the coating also of delicate substrates, which might even be liquid. The underlying mechanism is similar to free-radical polymerization processes,[14] where an initiator (typically, a peroxide) is decomposed into radicals at a heated filament, which interact with a monomer so that polymer synthesis is initiated, propagated by further monomer units until terminated by another radical. With the possibility of employing a plethora of chemical structures of the monomer, vast amounts of distinct polymers can be synthesized and conformally deposited onto three-dimensional (3D)-nanostructured substrates. For appli-

Received: August 1, 2019
Revised: August 30, 2019
Published: August 30, 2019

DOI: 10.1021/acs.jpcc.9b07340
J. Phys. Chem. C 2019, 123, 24165−24171

cations, the synthesis of smart polymer thin films is particularly interesting. Numerous polymers responding to variations in humidity, pH, salt, or solutes present in a solution have been developed.[15,16] For instance, temperature-responsive hydrogel encapsulations (e.g., poly(*N*-isopropylacrylamide)-based polymers, pNIPAAm) were reported to allow for the control of the release of drugs as a function of temperature; the release could even be slowed down at higher temperatures.[12] Cross-linking of the polymeric structures, for instance, by copolymerizing di(ethylene glycol) divinyl ether (DEGDVE) together with the monomer exhibiting the desired functionalities, enables the variation of the polymers' swelling behavior.[16,17] Recently, another interesting polymer, namely, poly(*N*-vinylcaprolactam) (pNVCL), has been synthesized by iCVD allowing for further tunability of the polymeric thermoresponsiveness. Importantly, this polymer is biocompatible, making it a promising candidate also for other medical applications, where coating might assist some purpose, i.e., abrasion or cell adhesion.

In this contribution, we study the wrinkle formation upon iCVD synthesis of a thermoresponsive polymer thin film (i.e., *p*(NVCL-*co*-DEGDVE)) directly onto another polymer, being Eudragit E100 (EUD). EUD is typically employed as a drug coating itself, adopting solution-based techniques; it is soluble at low pH and only swells at larger pH, typically above 5, making it usable as an enteric coating. On addition of the thermoresponsive pNVCL-based thin film, the temperature response can be tuned in potential applications. On the one hand, a superior coating might be achieved by the tunability in the thermoresponsiveness of pNVCL and the enteric properties of EUD. On the other hand, the larger surface area due to wrinkling might be used to alter the release behavior of the resulting structures, when used for encapsulation purposes.

EXPERIMENTAL METHODS

Single crystal silicon wafers (Siegert Wafers, Germany) with a native oxide layer were used as substrates. Substrates were prepared by cutting the wafers into 2 × 2 cm^2 pieces, sonicating them in EtOH and acetone baths, and, finally, drying under a nitrogen stream. An amino methacrylate copolymer with the tradename Eudgagit E100 from Evonik (Germany) is a coating material typically used in pharmaceutical applications. The material was used as delivered. For the sample preparation, the material was dissolved in toluene (Sigma-Aldrich, Germany) at different concentrations. Using a standard spin coater employing a spin speed of 17 rps for 60 s, this allowed to deposit homogeneous layers of EUD ranging in thickness between a couple of nm up to nearly 1 μm. The thickness of these layers was determined using a spectroscopic ellipsometer (M-2000S, J.A. Woollam). The measurements were performed in a wavelength range of 370−1000 nm at three angles (65/70/75°). The experimental data was fitted within the CompleteEASE software package by an optical model consisting of a Si semi-infinite layer on the bottom, a 1.6 nm thick native SiO_2 layer in the middle, and the EUD film on top. The substrate materials were modeled by the corresponding material files available within the software, and the EUD layer was modeled as a Cauchy function with an Urbach tail accounting for adsorption in the low-wavelength region.

Poly(*N*-vinylcaprolactam-*co*-di(ethylene glycol) divinyl ether) thin films were synthesized by initiated chemical vapor deposition. The depositions were run in a custom-built iCVD reactor described elsewhere.[17] *N*-Vinylcaprolactam (NVCL, 98%; Sigma-Aldrich, Germany) is used as the monomer and di(ethylene glycol) divinyl ether (DEGDVE, 99%; Sigma-Aldrich, Germany) as the cross-linker. NVCL and DEGDVE are delivered to the reactor from their individual glass jars held at elevated temperatures: 78 and 70 °C, respectively. The monomer flow rate (NVCL) is set to 0.2 sccm; the DEGDVE flow rate is varied to employ different amounts of cross-linking. The corresponding ratios of vapor pressures of the monomer and initiator to their saturation vapor pressures (p_M/p_{sat}) in the employed temperature and pressure conditions are considered for estimating the resulting compositions. All of the corresponding p_M/p_{sat} values are below 0.2 and, thus, lie in a range, where a linear relation to the surface concentration of the chemical species has been reported.[18] The applied flow rates yield polymer layers of *p*(NVCL-*co*-DEGDVE) with a nominal cross-linking of 20−85%, as evaluated from the ratio of employed p_M/p_{sat} values at a working pressure of 250 mTorr and a substrate temperature of 35 °C. A filament temperature of 200 °C was used for all presented depositions. To monitor the deposited thickness, in situ laser interferometry with a He−Ne laser (λ = 633 nm; Thorlabs) is performed through a removable quartz glass lid. All samples of the cross-linker series exhibit film thickness values of 100 ± 5 nm; moreover, a film thickness series with 45% of nominal cross-linking has been deposited with 10, 30, and 50 nm layer thicknesses.

Atomic force microscopy (AFM) measurements were performed using a FlexAFM (Nanosurf, Switzerland) equipped with a C3000 controller. The tapping mode measurements were performed using a Tap300-Al from BudgetSeonsors (Bulgaria). Data processing and analysis were performed using the software package Gwyddion.[19] For the extraction of the roughness, the implemented statistic evaluation was used, from which its uncertainty was also estimated. As the wrinkles are randomly oriented in a lateral dimension, a simple line-scan analysis cannot be performed. Therefore, we used a two-dimensional (2D) fast Fourier transform of the AFM height data. From this calculation, we evaluated the radial information by summing over distances from zero and fitting a Lorentzian function to it to extract the peak position that corresponds to the wrinkle wavelength. The uncertainty of fitting yields the uncertainty for the wavelength extracted.

RESULTS AND DISCUSSION

Spacer Thickness Dependence. Eudragit (EUD) is readily soluble in various solvents up to high amounts. This makes it possible to use techniques like spin coating for the deposition of homogeneous thin films, e.g., on silicon wafer substrates. By applying different polymer concentrations, fully closed EUD thin films with thicknesses ranging from 20 to 800 nm, as determined by spectroscopic ellipsometry, were prepared. The resulting layers are amorphous and, if touched, sticky; the films are very smooth so that AFM analysis did not reveal any structural features.

On top of such an amorphous EUD layer, an additional polymer layer can be directly synthesized by iCVD. For a first set of samples, we deposited 100 nm *p*(NVCL-*co*-DEGDVE) with a cross-linker content of 35%. Thin EUD films (up to 40 nm) coated by the iCVD layer show a rather smooth and homogeneous morphology (see Figure 1, top left). Small spots of 5 nm in height exhibiting radii of about 100 nm are also observable but appear less frequent. In fact, these kinds of structures are only present when the EUD layers are thin. In a

DOI: 10.1021/acs.jpcc.9b07340
J. Phys. Chem. C 2019, 123, 24165−24171

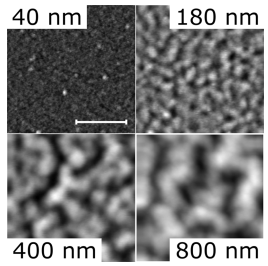

Figure 1. Exemplary atomic force microscope images of wrinkle formation of various EUD−iCVD double layers; the thickness of the EUD film was varied (as indicated in the pictures), while the thickness of the 35% cross-linked iCVD thin film was kept constant at 100 nm (the scale bar indicates 2 μm and applies for all images; individual gray scales for heights).

recent study using iCVD-deposited poly(2-hydroxyethyl methacrylat) (pHEMA) as an encapsulation for drug layers, a very similar behavior has been observed, i.e., particle-like structures concomitantly being present with rather smooth areas.[11] Using thicker EUD layers of 100 nm, the onset of wrinkle formation on the sample surface can be observed, while the mentioned spots are hardly noticeable anymore (see Figure 1, top right).

The evaluation of such surfaces can be performed in various ways. Here, the root-mean-square roughness σ_{rms} and the lateral wavelength of the structures λ, both calculated directly from the AFM height data, are plotted in Figure 2. For

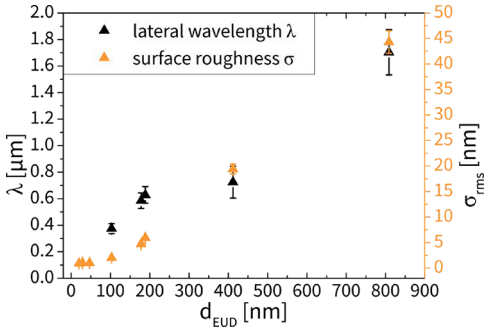

Figure 2. Development of the root-mean-square roughness σ_{rms} of an EUD−iCVD double-layer system (35% cross-linked) as evaluated by AFM as a function of the EUD layer thickness d_{EUD}; the lateral wavelength of the structures λ was evaluated for the same samples from a 2D fast Fourier transform and is plotted on the right y-axis.

statistical reasons, these data were determined from scans of larger size (up to 50 × 50 μm^2), while the data in Figure 1 elucidate more details on a smaller scale. For samples of a 100 nm EUD thickness or less, the small structures reflected in the roughness value remain comparably small; a root-mean-square roughness of σ_{rms} = 2 nm or below was identified. For these samples of low EUD thickness, the evaluation of the lateral wavelength from the AFM data was not unambiguously possible due to the low roughness and the random statistical nature of the surface structure.

At a 180 nm EUD thickness, the morphology appears to be different and the formation of pronounced wrinkles is observed. The evaluation of the surface roughness shows an increase to around σ_{rms} = 6 nm. For these samples, the evaluation of the wrinkle wavelength reveals more precise and regular information and an average lateral size of about 600 nm could be extracted. It can be noted that, to a certain extent, σ_{rms}, determined here by the software, represents the amplitude of the structures (i.e., a measure for the deviation up and down from an average height).

For samples prepared from even thicker EUD layers, the situation remains similar, with homogeneous wrinkles being present on the entire surface; the surface roughness and lateral size of the apparent structures increase proportionally to the film thickness of the EUD layer (see Figure 2). For an EUD layer of 800 nm, the roughness increases to a maximum value of 45 nm. On the same sample, a lateral structure with a wavelength of about 1.6 μm developed. The shallowness of these structures, apparent when comparing the thickness of the layer of about 900 nm (EUD and iCVD) to the relatively low roughness of 45 nm, suggests that the character of the wrinkles is more two-dimensional rather than fully 3D down to the substrate surface.

Cross-Linker Density. Besides the spacer thickness dependence, the observed wrinkle formation has also been studied as a function of cross-linking of the *p*(NVCL-*co*-DEGDVE) coating. By employing the iCVD technique for the synthesis of thin films, one can easily adjust the amount of cross-linking by changing the cross-linker flow rate during synthesis. This can have various effects on the film's performance. For instance, a cross-linking agent prevents the thin film from delaminating from the substrate when in contact with water. *p*(NVCL-*co*-DEGDVE) thin films deposited by iCVD were reported to be stable above 10% cross-linking.[20] Further, cross-linking alters the swelling response of the hydrogel layer drastically when in contact with water or just specifically humid environments.[17,20] In medical or drug applications, this enables the tunability of release profiles of a drug out from an iCVD encapsulation with the dissolution rate being adjustable by orders of magnitude.[12] In the present contribution, we study the impact of the cross-linker amount used in iCVD synthesis on the film morphology, when deposited onto EUD films. In Figure 3, exemplary AFM images of samples with about 400 nm EUD spacers coated by 100 nm *p*(NVCL-*co*-DEGDVE) thin films with varying cross-linker amounts are summarized.

For the sake of direct comparability, the average dark/brightness of the images in Figure 3 gives an indication on the roughness of the structures using the exact same height scale of 250 nm for all images. Upon inspection, the overall roughness

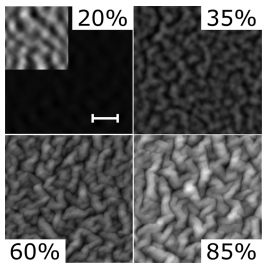

Figure 3. AFM height images of samples with 400 nm EUD layers coated with various differently cross-linked 100 nm *p*(NVCL-*co*-DEGDVE) thin films (20−85% as indicated in the images). The scale bar represents 2 μm and applies for all images; the same gray scale for heights ranging from 0 to 250 nm (black to weight). For a region of the image of a 20% cross-linked sample (top left), the maximum of the gray scale/white was adjusted to 25 nm enhancing the visibility of surface structures.

DOI: 10.1021/acs.jpcc.9b07340
J. Phys. Chem. C 2019, 123, 24165−24171

appears to increase with increasing the amount of cross-linking from 20% (top left) to 85% (bottom right). The low surface roughness (σ_{rms} = 4 nm) of the 20% cross-linked sample indicates a rather flat homogeneous surface. When a part of the image of the 20% cross-linked sample (top left) is adjusted in the height scale (see the inset), additional features appear, which are very similar to those observed when the onset of wrinkling is not entirely reached yet (cf. Figure 1). For the same EUD layer thickness of about 400 nm, a sample coated with a cross-linking density of 35% clearly shows the presence of wrinkles; a roughness of about 20 nm was found, which is about 5 times higher than the 20% cross-linked system was able to induce. At cross-linking contents of 60 and 85%, large wrinkles develop, with the roughness increasing to 30 and 36 nm, respectively. In general, a change in morphology is often observed in different stages of wrinkling.[5,21] For instance, in the present contribution, the morphology of the wrinkles appears to be more round/hexagonal and very shallow for low amounts of cross-linking. When the cross-linker amount is increased, the situation changes toward more elongated wrinkles also exhibiting more pronounced height variations.

The surface roughness (σ_{rms}) as evaluated from the AFM data as a function of the spacer thickness (EUD coating) for various differently cross-linked *p*(NVCL-*co*-DEGDVE) systems can be found in Figure 4. For low EUD spacer thickness

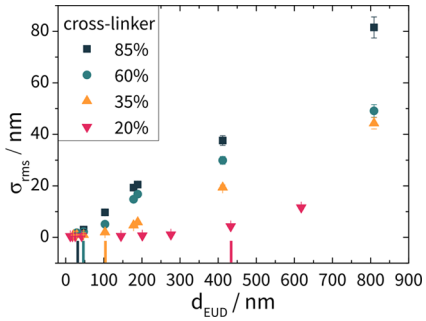

Figure 4. Root-mean-square surface roughness (σ_{rms}) as a function of the spacer thickness (EUD) for various samples coated with 100 nm *p*(NVCL-*co*-DEGDVE) thin films with varying amounts of cross-linking as given in the legend; the onset thickness of wrinkle formation as evaluated by the morphology of the films is indicated at the *x*-axis as dashes for the respectively cross-linked systems (matching colors).

(below 30 nm), similar surface roughness values (below 2 nm) were evaluated for all deposited cross-linker amounts. The surface morphology does not indicate wrinkle formation in that film thickness regime. Above 30 nm of EUD, the differently cross-linked polymer thin films lead to a strong dependence of the surface roughness on the spacer layer thickness, but each cross-linker amount results in distinct behavior. As already shown for the samples with a 400 nm spacer layer thickness (see Figure 3), the data in Figure 4 reveals that the surface roughness increases with increasing the cross-linker amount of the hydrogel in all of the range of investigated spacer layer thicknesses. From the respective AFM data, also the onsets (minimum spacer thickness values) of wrinkle formation as a function of cross-linking were evaluated. As an indication, one can see the significant change in morphology (from homogeneous to wrinkled) observable in the AFM height images. Nevertheless, for statistical reasons, another approach is used: at small spacer thickness, the samples appear to have a rather similar and homogeneous morphology exhibiting surface roughness values around 1 nm. At higher thickness, the surface roughness appears to depend linearly on the spacer layer thickness with increasing slopes for increasing cross-linker amounts. Using this second regime, extrapolation to zero surface roughness by linear regression fits shows that the onset of wrinkling is taking place at around 320 nm spacer thickness when the cross-linker is just 20%. Increasing the cross-linker amount, the onset shifts to 100 nm (at 35% cross-linker), 50 nm (at 60% cross-linker), and down to about 40 nm for the largest density of cross-linking (85%).

Again, the lateral wavelength of the wrinkles (λ) was determined from a 2D fast Fourier transform of the AFM data and plotted in Figure 5a for the differently cross-linked

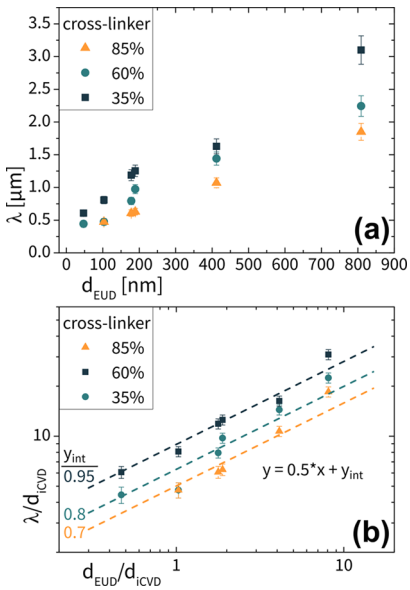

Figure 5. (a) Wavelength λ as evaluated from the AFM height images of differently cross-linked (35, 60, and 85%) *p*(NVCL-*co*-DEGDVE) layers of 100 nm thickness (d_{iCVD}) deposited on EUD layers of different thickness (d_{EUD}); (b) plot for the evaluation of the ratio of iCVD to EUD elastic modulus for the differently cross-linked systems from linear fits of the plotted data (respective intercept with the *y*-axis, y_{int}).

samples. Thin spacer layers and low amounts of cross-linking do not result in significant wrinkling and, thus, unambiguous wavelength determination. Hence, the relatively small roughness of the samples with 20% nominal cross-linking did not allow for a determination of the wrinkle wavelength. For all of the other investigated samples, λ steadily increases with increasing the spacer thicknesses.

In the literature, there are several great examples of how the size of such wrinkles can be explained. For our previous work, when the iCVD layer was deposited on an amorphous drug layer made from clotrimazole, we used a model assuming a stiff film on a compliant substrate of similar thickness. For the case of an incompressible substrate (i.e., here EUD), an analytical expression can be derived, which relates the wrinkle wavelengths (λ), the thicknesses (d), and the elastic moduli (E) of the components

$$\frac{\lambda}{2\pi \times d_{iCVD}} = \sqrt{\frac{d_{EUD}}{d_{iCVD}}} \left(\frac{E_{iCVD}}{18 \times E_{EUD}} \right)^{1/6}$$

DOI: 10.1021/acs.jpcc.9b07340
J. Phys. Chem. C 2019, 123, 24165−24171

From a double-logarithmic plot of the normalized experimental data[11] (i.e., $\frac{\lambda}{d_{iCVD}}$ over $\frac{d_{EUD}}{d_{iCVD}}$), the ratio of the elastic moduli of the iCVD layer (E_{iCVD}) and the EUD layer (E_{EUD}) was determined from the intercept of the linear fit of the respective data with slope 0.5 with the y-axis (y_{int}, see Figure 5b). The respective ratios are calculated by the following formula

$$\frac{E_{iCVD}}{E_{EUD}} = 18 \times \left(\frac{10^{y_{int}}}{2\pi}\right)^6$$

Performing the evaluation of the samples with 85% nominal cross-linking reveals that the elastic modulus of the iCVD layer is about 128 times larger than the one of the underlying EUD layers. In a previous contribution, we estimated the apparent elastic moduli of differently cross-linked *p*(NVCL-*co*-DEGDVE) thin films swollen in water to lay between 5 and 120 MPa, with E increasing with cross-linking.[20] The elastic modulus in air is expected to be at least 1 order of magnitude higher and should, thus, be in a range as for most polymers (e.g., polystyrene about 3.8 GPa within films).[22] The elastic modulus of EUD is unknown, but 128 times higher elasticity would suggest that the material is in a rubbery state with a rather low E-value. As the substrate temperature was held at 35 °C during iCVD synthesis and the EUD possesses a T_g of around 45 °C[23] with a typical layer thickness dependence of the T_g,[24] this might support this estimation.

For the samples with 60 and 35% cross-linker amounts, the elastic modulus ratios were determined to be 18 and 5, respectively. The magnitude of the range of values appears to be consistent with the assumption that the amount of cross-linking is directly related to the elastic modulus. This assumption has been proven to be present in the swollen state of differently cross-linked *p*(NVCL-*co*-DEGDVE) thin films.[20]

In general, for the wrinkling to take place, at least two slabs of materials with deviating properties need to be in contact. Strain in the system or differences in the mechanical properties can induce wrinkling. In the case of the investigated EUD–iCVD double layers, it can be assumed that the EUD is rather relaxed with minimum or even absent strain after the spin-coating process in its amorphous state. Upon iCVD synthesis, the monomers and the initiator radicals arrive at the substrate and adsorb at the EUD–air interface. Eventually, initiator radicals attack the vinyl bonds of the adsorbed species, which leads to polymerization of these monomer units. As the components are highly reactive, the synthesis is a rather fast process and just limited by the amount of material being present on the substrate in the applied conditions. As such, the time for adapting to low energetic steric sites is limited, causing the material to evolve in a strained state. With the strain exceeding the mechanical strength of the underlying EUD layer, wrinkling will be induced. The amount of wrinkling is then dependent on the amount of strain and the difference in the elastic moduli of the materials involved. High cross-linking of the iCVD polymer causes a higher rigidity, resulting in a reduced capability of adapting to steric limitations and, thus, more strain might be introduced by applying more cross-linked polymers. In a similar manner, having differences in the amount of cross-linking changes the chemical appearance, which, for instance, alters the surface energy of the deposited material. This is reflected in the (advancing) water contact angle changing from below 70° for 75% cross-linked *p*(NVCL-*co*-DEGDVE) thin films up to more than 80° for lower cross-linker amounts, as just recently determined.[20] Thus, the hydrophilic cross-linker reduces the hydrophobicity. As there was no change in the EUD layer surface, this change can result in a different energetic contribution (difference in surface energies) and superimpose the strain developing during deposition.[25]

iCVD Thickness Dependence. Intuitively, one follow-up question arises: is the induced strain already present at the beginning of the deposition, i.e., in the first nanometers, or does it vary with layer thickness of the iCVD film? To evaluate these considerations, several depositions (all being 45% cross-linked) exhibiting different iCVD thicknesses were carried out on similar EUD layers with varying thicknesses. Again, an AFM analysis has been carried out on the different systems; AFM height images are shown in Figure 6. As described earlier,

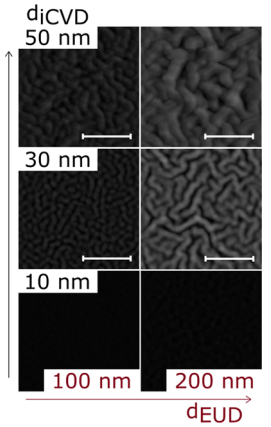

Figure 6. AFM height images of samples with 100 and 200 nm EUD layers coated with various differently thick *p*(NVCL-*co*-DEGDVE) thin films (10, 30, and 50 nm); the scale bars indicate 2 μm and apply for all images; the gray scale corresponding to heights is defined in the range of 0–200 nm (black to white).

wrinkle formation appears to yield more pronounced wrinkles with larger lateral wavelengths, when the iCVD thin film is deposited on thicker EUD layers. At a 10 nm iCVD top layer film thickness, no distinct surface morphology and, hence, no wrinkle formation could be identified (see Figure 6 bottom); the surface roughness remains at the value of the underlying layer of around 1 nm. At a 30 nm top layer thickness, wrinkles start to appear. They are similarly pronounced in height when compared to the 50 nm thick films as the surface roughness (σ_{rms}) is around 7 nm for the 30 and 50 nm films deposited on top of the 100 nm EUD layer. Correspondingly, σ_{rms} remains at around 13 nm, no matter if 30 or 50 nm of iCVD film is deposited on the 200 nm EUD layers. However, the wrinkles seem to grow in the lateral dimension between 30 and 50 nm of the deposited iCVD polymer. For the deposition on top of the 100 nm EUD layers, the lateral wavelength of the wrinkles (λ) increases from 0.3 μm for 30 nm of deposition to 0.6 μm for 50 nm. For the 200 nm EUD layers, the situation is similar, whereas λ was determined to be 0.5 μm for 30 nm of the iCVD polymer and 1 μm for 50 nm.

As can be seen by comparing the AFM height images in the middle and top of Figure 6, the top layer thickness can also be used to alter the resulting wrinkle morphology. As for 30 nm of iCVD layer thickness, rather homogeneous wrinkled structures

DOI: 10.1021/acs.jpcc.9b07340
J. Phys. Chem. C 2019, 123, 24165–24171

can be observed; the 50 nm samples appear to be more chaotic/inhomogeneous in terms of morphological diversity.

CONCLUSIONS

Wrinkling phenomena might be used in a variety of different fields. For the induction, often, prestrain is required. Wrinkling can directly be observed when the iCVD polymer is synthesized on top of another polymer layer, here made from EUD. For such a purpose, the lack of solvents used in iCVD is particularly advantageous. Changing the thickness of the underlying layer results in the ability to adjust the wrinkles induced in terms of morphology. Both the surface roughness (as a measure of the amplitude) and the wrinkle wavelength increase with increasing the spacer thickness, whereas the absolute value of the wavelength is always much larger than that of the amplitude. While this suggests that this is an effect, especially altering the surface of the layers, the variation in spacer thickness changing the surface structure over a large range of employed thicknesses hints toward a more general rearrangement of the entire layers. The iCVD technique is very versatile so that parameters like the flow rates can be used to tailor the properties of the deposited iCVD layers in a wide range of directions. The results here show that variation in cross-linker amount affects the onset of wrinkling and the wrinkle morphology. It can be expected that further variation in the iCVD process would also result in the further tunability of the resulting wrinkles in the investigated systems; among others, deposition rate, substrate temperature, or filament temperature might be varied easily, resulting in altered polymer properties. In a similar manner, different substrates can be employed to alter the wrinkling. While not shown here, stiff materials like PS or PMMA did not allow for the development of wrinkles upon applying *p*(NVCL-*co*-DEGDVE) thin films on top, while EUD even facilitates their extensive tunability. The addition of a material into the EUD polymeric film matrix (like a plasticizer) enables even further possibilities to change the wrinkling behavior. Having such possibilities, applications like light diffusion in solar cells or even surface enlargement in medication might be re-engineered to outperform established systems.

AUTHOR INFORMATION

Corresponding Author

*E-mail: fmuralter@tugraz.at.

ORCID

Fabian Muralter: 0000-0001-8038-6019

Anna Maria Coclite: 0000-0001-5562-9744

Oliver Werzer: 0000-0003-0732-4422

Notes

The authors declare no competing financial interest.

ACKNOWLEDGMENTS

This project has received funding from the European Research Council (ERC) under the European Union's Horizon 2020 research and innovation program (grant agreement 715403).

REFERENCES

(1) Kim, J. B.; Kim, P.; Pégard, N. C.; Oh, S. J.; Kagan, C. R.; Fleischer, J. W.; Stone, H. A.; Loo, Y.-L. Wrinkles and Deep Folds as Photonic Structures in Photovoltaics. *Nat. Photonics* **2012**, *6*, 327−332.

(2) Ryu, S. Y.; Seo, J. H.; Hafeez, H.; Song, M.; Shin, J. Y.; Kim, D. H.; Jung, Y. C.; Kim, C. S. Effects of the Wrinkle Structure and Flat Structure Formed During Static Low-Temperature Annealing of ZnO on the Performance of Inverted Polymer Solar Cells. *J. Phys. Chem. C* **2017**, *121*, 9191−9201.

(3) Chaieb, S.; Natrajan, V. K.; El-rahman, A. A. Glassy Conformations in Wrinkled Membranes. *Phys. Rev. Lett.* **2006**, *96*, No. 078101.

(4) Cerda, E.; Mahadevan, L. Geometry and Physics of Wrinkling. *Phys. Rev. Lett.* **2003**, *90*, No. 074302.

(5) González-Henríquez, C. M.; Sarabia Vallejos, M. A.; Rodríguez-Hernández, J. Strategies for the Fabrication of Wrinkled Polymer Surfaces. In *Wrinkled Polymer Surfaces*; Springer International Publishing: Cham, 2019; Vol *14*, pp 19−59.

(6) Kato, M.; Tsuboi, Y.; Kikuchi, A.; Asoh, T.-A. Hydrogel Adhesion with Wrinkle Formation by Spatial Control of Polymer Networks. *J. Phys. Chem. B* **2016**, *120*, 5042−5046.

(7) Awaja, F.; Zhang, S.; Tripathi, M.; Nikiforov, A.; Pugno, N. Cracks, Microcracks and Fracture in Polymer Structures: Formation, Detection, Autonomic Repair. *Prog. Mater. Sci.* **2016**, *83*, 536−573.

(8) Chung, J. Y.; Douglas, J. F.; Stafford, C. M. A Wrinkling-Based Method for Investigating Glassy Polymer Film Relaxation as a Function of Film Thickness and Temperature. *J. Chem. Phys.* **2017**, *147*, No. 154902.

(9) Gao, N.; Zhang, X.; Liao, S.; Jia, H.; Wang, Y. Polymer Swelling Induced Conductive Wrinkles for an Ultrasensitive Pressure Sensor. *ACS Macro Lett.* **2016**, *5*, 823−827.

(10) Gu, J.; Li, X.; Ma, H.; Guan, Y.; Zhang, Y. One-Step Synthesis of PHEMA Hydrogel Films Capable of Generating Highly Ordered Wrinkling Patterns. *Polymer* **2017**, *110*, 114−123.

(11) Christian, P.; Ehmann, H. M. A.; Werzer, O.; Coclite, A. M. Wrinkle Formation in a Polymeric Drug Coating Deposited via Initiated Chemical Vapor Deposition. *Soft Matter* **2016**, *12*, 9501−9508.

(12) Christian, P.; Tumphart, S.; Ehmann, H. M. A.; Riegler, H.; Coclite, A. M.; Werzer, O. Controlling Indomethacin Release through Vapor-Phase Deposited Hydrogel Films by Adjusting the Cross-Linker Density. *Sci. Rep.* **2018**, *8*, No. 7134.

(13) Christian, P.; Ehmann, H. M. A.; Coclite, A. M.; Werzer, O. Polymer Encapsulation of an Amorphous Pharmaceutical by Initiated Chemical Vapor Deposition for Enhanced Stability. *ACS Appl. Mater. Interfaces* **2016**, *8*, 21177−21184.

(14) Lau, K. K. S.; Gleason, K. K. Initiated Chemical Vapor Deposition (ICVD) of Poly(Alkyl Acrylates): An Experimental Study. *Macromolecules* **2006**, *39*, 3688−3694.

(15) Chu, L. Y.; Xie, R.; Ju, X. J.; Wang, W. Smart Hydrogel Functional Materials. In *Smart Hydrogel Functional Materials*; Springer: Heidelberg New York Dordrecht London, 2013; Vol. *V*−*XVIII*, pp 1−381.

(16) Pena-Francesch, A.; Montero, L.; Borrós, S. Tailoring the LCST of Thermosensitive Hydrogel Thin Films Deposited by ICVD. *Langmuir* **2014**, *30*, 7162−7167.

(17) Muralter, F.; Perrotta, A.; Coclite, A. M. Thickness-Dependent Swelling Behavior of Vapor-Deposited Smart Polymer Thin Films. *Macromolecules* **2018**, *51*, 9692−9699.

(18) Lau, K. K. S.; Gleason, K. K. Initiated Chemical Vapor Deposition (ICVD) of Poly(Alkyl Acrylates): A Kinetic Model. *Macromolecules* **2006**, *39*, 3695−3703.

(19) Nečas, D.; Klapetek, P. Gwyddion: An Open-Source Software for SPM Data Analysis. *Cent. Eur. J. Phys.* **2012**, *10*, 181−188.

(20) Muralter, F.; Perrotta, A.; Werzer, O.; Coclite, A. M. Interlink between Tunable Material Properties and Thermo-Responsiveness of Cross-Linked Poly(*N*-Vinylcaprolactam) Thin Films Deposited by Initiated Chemical Vapor Deposition. *Macromolecules* **2019**, DOI: 10.1021/acs.macromol.9b01364.

(21) Guvendiren, M.; Burdick, J. A. The Control of Stem Cell Morphology and Differentiation by Hydrogel Surface Wrinkles. *Biomaterials* **2010**, *31*, 6511−6518.

DOI: 10.1021/acs.jpcc.9b07340
J. Phys. Chem. C 2019, 123, 24165−24171

(22) Miyake, K.; Satomi, N.; Sasaki, S. Elastic Modulus of Polystyrene Film from near Surface to Bulk Measured by Nanoindentation Using Atomic Force Microscopy. *Appl. Phys. Lett.* **2006**, *89*, No. 031925.
(23) Jadhav, N. R.; Gaikwad, V. L.; Nair, K. J.; Kadam, H. M. Glass Transition Temperature: Basics and Application in Pharmaceutical Sector. *Asian J. Pharm.* **2009**, *3*, 82−89.
(24) Fryer, D. S.; Peters, R. D.; Kim, E. J.; Tomaszewski, J. E.; de Pablo, J. J.; Nealey, P. F.; White, C. C.; Wu, W. L. Dependence of the Glass Transition Temperature of Polymer Films on Interfacial Energy and Thickness. *Macromolecules* **2001**, *34*, 5627−5634.
(25) Huang, R.; Stafford, C. M.; Vogt, B. D. Wrinkling of Ultrathin Polymer Films. *MRS Proc.* **2006**, *924*, 0924−Z04-10.

NOTE ADDED AFTER ASAP PUBLICATION

This paper was published ASAP on August 30, 2019, and due to a production error the Figure 2 graphic was incorrect. The corrected version was reposted on September 18, 2019.

DOI: 10.1021/acs.jpcc.9b07340
J. Phys. Chem. C 2019, 123, 24165−24171